A multiscale slice model for continuous casting of steel

B Šarler[1,4], **R Vertnik**[1,2], **A Z Lorbiecka**[1], **I Vušanović**[3] **and B Senčič**[2,4]

[1] Laboratory for Multiphase Processes, University of Nova Gorica, Vipavska 13, SI-5000, Nova Gorica, Slovenia.
[2] Štore Steel d.o.o, Technical Developement, Železarska 3, SI-3220 Štore, Slovenia.
[3] Faculty of Mechanical Engineering, University of Montenegro, George Washington st., 81000 Podgorica, Montenegro.
[4] Centre of Excellence for Biosensorics, Automation and Process Control, Velika pot 22, Solkan, Slovenia.

E-mail: bozidar.sarler@ung.si, robert.vertnik@store-steel.si, alorbiecka@ung.si, bojan.sencic@store-steel.si

Abstract. A simple Lagrange-an traveling slice model has been applied for the prediction of the relations between process parameters, macrosegregation and solidification grain structure formation (equiaxed to columnar and columnar to equiaxed transition) during the continuous casting process of steel billets. The main advantage of the slice model is its very fast calculation time in comparison with the complete 3D heat and fluid flow model which might need calculation time, measured in days. The slice models thus allows for fast optimisation and even for on-line simulation. The heat and species transfer models are based on the mixture continuum assumptions with Lever solidification rule and enhanced thermal and solutal diffusivities for heuristic accounting of fluid flow effects. The grain structure evolution model is based on the Gaussian nucleation rule, and KGT growth model, coupled to the macroscopic heat and species transfer models. The heat and species transfer models are solved by the meshless technique by using local collocation with radial basis functions. The grain structure evolution model is solved by the point automata technique, a novel meshless variant of the cellular automata method. A comparison of the results with the experimental data for steel grade 51CrV4 is shown in terms of macrosegregation and grain structure across the billet. Simulations and comparisons have been carried out for nominal casting conditions, reduced casting temperature, and reduced casting speed. The model predicts surprisingly well the qualitative features of the macrosegregation and grain structure patterns. Possible refinements of the model with respect to other physical mechanisms are discussed.

1. Introduction

Continuous casting [1] is currently the most common process for production of steel. The process can be accompanied by a range of quality problems such as shape defects, cracking, inclusions, non-uniform microsegregation, macrosegregation, porosities, etc. Respectively, there is a very big demand for related process modeling, which is used in the design of casters, proper setting of process parameters, and on-line control of the casters. The models [2] range from very simple, usually used in the on-line mode in the regulation of the plant, to very sophisticated multiscale and multiphysics approaches that run off-line for several days and tackle the specific aspects of the process like melt – casting powder interaction, inclusions dynamics, oscillation mark formation, etc. The focus in this

paper is the so called slice model. This model neglects all interactions in the direction of the casting, and takes into account only the interactions perpendicular to the casting in form of a traveling slice. Respectively, a quasi-three dimensional picture of the strand status can be obtained much faster than when solving a complete 3D configuration. This model [3,4] performs well for heat transfer, but of course could not predict any realistic [5] turbulent fluid flow effects. Several important solidification [6] parameters, such as the shell thickness along the casting direction, the metallurgical length and the temperature of the strand surface can be calculated satisfactory accurate. Recently, the slice model has been upgraded with the solution of the grain structure [7] and macrosegregation [8] for simple Fe-C steel. The macrosegregation has been taken into account by assuming the enhanced thermal diffusivity of the liquid phase. Both, the simple grain structure and the simple macrosegregation model predict surprisingly well the qualitative features of the strand. It is the purpose of this paper to upgrade the simple slice model for estimating the grain structure and the macrosegregation in the strand to multicomponent steel. We are aware that the quantitative picture, obtained from such a simple model, might be too crude, however, on the other hand, such a simple model can be used in the on-line mode and give the plant operators a quick insight into the quality changes and trends in the strand as a function of the process parameter changes.

2. Slice model assumptions

A schematics of the continuously cast strand is shown in figure 1 with shaded traveling slices. The temperature and the concentration field of the slice can be computed from known time dependent boundary conditions. The slice time is on the other hand associated with the position in the strand. The Cartesian coordinate z measures the length from the meniscus. The strand geometry is assumed straightened along this coordinate, which is a geometrical simplification of the real curved casting process. In all slice models the mass, heat, momentum, and solute transfers in the casting direction are neglected. The z coordinate can thus be considered parabolic, while the x and y coordinates are elliptic. In this way all fields at a given z coordinate depend only on the slice history, including its cooling intensity as a function of time. The slices form at the z_{start} longitudinal coordinate of casting and travel in the direction of the $\mathbf{i}_z$ base vector with the casting speed $\mathbf{V}_{cast}$, (see figure 1). For calculating the cooling intensity of the slice as a function of time, a connection between the z coordinate of the casting machine and the slice history t is needed, which is in general:

$$z(t) = \int_{t_{start}}^{t} V_{cast}(t') \cdot dt' + z_{start}, V_{cast}(t) = \mathbf{V}_{cast}(t) \cdot \mathbf{i}_z \tag{1}$$

where t_{start} represents the initial time of a slice. In the case when the casting speed and other process parameters are steady, we obtain the following simple connection between the z coordinate of the casting machine and the slice history $t(z) = t_{start} + (z - z_{start}) / V_{cast}$.

3. Macroscopic transport model

3.1. Governing equations

A well-known continuum mixture model [9] is applied for solving the temperature and concentration of multicomponent steel in this study. It is assumed, consistently with the slice model postulates, that the macroscopic transport occurs only in travelling *x–y* cross sectional slice, moving from the top (horizontal position of slice) to the exit of casting rig (vertical position of slice) as seen on figure 1. The coordinate system is fixed with the slice, while the temperature and the boundary conditions are assumed as time dependent, based on constant casting speed and position of slice from the top to the bottom.

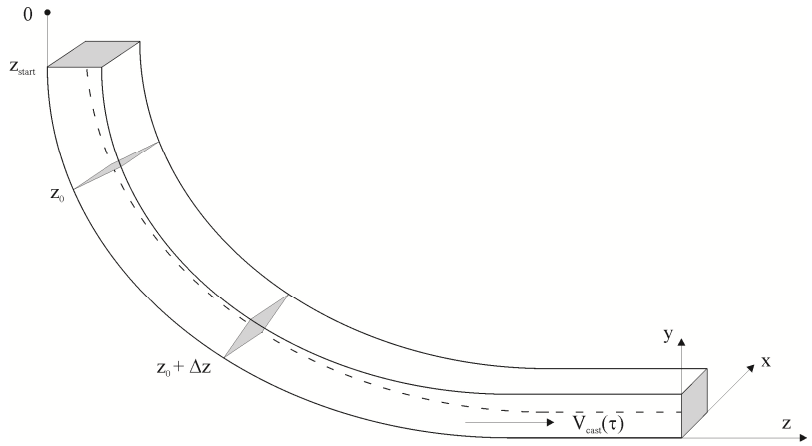

Figure 1. Slice traveling schematics in the strand.

The boundary temperatures of the travelling slice were obtained from the Robin type energy balance equations for slice boundaries, defined by the known heat transfer coefficients, and the temperature of the cooling fluid. Let us assume steel with N alloying elements. The related governing equation for heat and N equations for species transport are:

$$\frac{\partial}{\partial t}(\rho h) = \nabla \cdot (k \nabla T),\ \frac{\partial}{\partial t}(\rho C_n) = \nabla \cdot (\rho f_L D_{Ln} \nabla C_n) + \nabla \cdot \left(\rho f_L D_{Ln} \nabla (C_{Ln} - C_n)\right);\ n = 1,...,N \qquad (2,3)$$

where T stands for temperature, and the mixture quantities of steel (density $\rho = g_S \rho_S + g_L \rho_L$, thermal conductivity $k = g_S k_S + g_L k_L$, mixture enthalpy $k = f_S h_S + f_L h_L$, and mixture concentration $C_n = f_S C_{Sn} + f_L C_{Ln}$) were defined by using appropriate solid and liquid properties, weighted with either mass (f_S, f_L) or volume (g_S, g_L) fractions of solid S and liquid L phase.

3.2. Microsegregation model

In order to calculate the local temperature and liquid concentration of alloying elements, which is the driving force for macrosegregation, a supplementary microsegregation model is necessary. The supplementary microsegregation model calculates temperature *T*, solid C_S and liquid C_L concentrations, and mass fractions of solid f_S and liquid phase f_L as well. Mixture enthalpy and concentrations from the macro model (2,3) were used as input parameters for the micro model and they vary in general, while the solidification proceeds. In this study, simple Lever rule has been used. The governing equations for the supplementary microsegregation model are as follows:

- Mixture and phase enthalpies:

$$h = f_L h_L + f_S h_S;\ h_L = c_L T + (c_S - c_L) T_{sol} + h_f;\ h_S = c_S T, \qquad (4)$$

- Mixture concentration, lever rule concentration balance, liquidus temperature

$$C_n = f_L C_{Ln} + (1 - f_L) C_{Sn},\ C_{Sn} = k_n C_{Ln},\ T = T_M + \sum_{n=1}^{N} m_{Ln} C_{Ln}, \qquad (5)$$

where T_{sol}, and h_f are solidus temperature and latent heat of phase change, k_n and m_{Ln} are the partition coefficients and the liquidus slopes of the alloying components (n=C, Cr, Ni). The influence of the turbulent fluid flow on macrosegregation is taken into account through the artificially increased liquid diffusivity (D_L=$50D_{nom}$).

3.3. Geometry, material properties, boundary and initial conditions

In this study, a quadratic shape of traveling slice is used with dimensions L_x = L_y = 0.14 m. The physical properties are $\rho_{S(L)}$=7870(6990) kg/m^3, $c_{S(L)}$=824.9(1395.8) J/kgK, $k_{S(L)}$=25(39.9) W/mK, and h_f = 2.711x10^5 J/kg. The diffusion coefficient in the solid is neglected in this study, since it is more than one order of magnitude lower compared to the liquid one. The initial conditions for traveling slice in this study are determined by the inlet superheat ΔT_{in} = 20 K and initial uniform concentration of alloying Carbon, Chromium and Nickel respectively: C_C = 0.51 wt%, C_{Cr} = 1.091 wt%, C_{Ni}=0.105wt% (main alloying components of steel 51CrV4). The heat flow from the slice to the cooling liquid is determined through the heat transfer coefficients: h_{mold} = 2000 W/m^{2}K for the mold section until z = 0.8 m, and h_{spray} = 800 W/m^{2}K for the spray cooling section until the end of casting machine (z = 10.8 m). The reference cooling water temperature in Robin boundary conditions is set to T_{ref} = 30 ^{o}C. The casting speed is V_{cast} = 1.75 m/min. The explicit time discretization step length in this study is set to Δt = 0.1 s for temperature and concentration calculations.

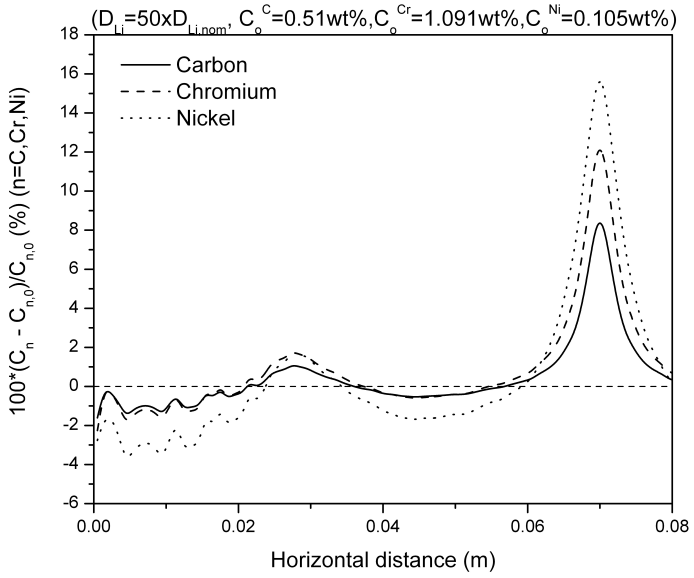

Figure 2. Calculated macrosegregation of C, Cr and Ni through the center (at 0.07 m) of the billet, parallel with the side.

The denominated horizontal cross section profiles of alloying carbon, chromium and nickel of the Fe-0.51wt%C-1.091wt%Cr-0.105wt%Ni steel, depicted in figure 2, were calculated by assuming the simple Lever rule for calculation of local temperature, phase fractions, and compositions. For all three elements there is a negative segregation near the surface, followed by a possitive segregation arround 3 cm from surface and then negative, and finally peak positive centreline segregation. The peak at approximately 0.03 m appears in the model due to the change of heat flux on the boundary from mould to the spray cooling region. This behaviour is in line with the experimental observations. However, equations (2-3) with artificially increased liquid diffusivity of course represent a quite rough approximation to the real and complex fluid flow pattern and deformation of the mushy zone. Increased diffusion on the macro scale reflects on the micro level as accelerated freezing in the mushy zone, and lower solid composition.

4. Grain structure model

Most of the grain growth models focus on the binary alloys [10, 11] and very little attention is focused to multicomponent alloys [12]. In this section a general theoretical model is discussed to describe the CET/ECT growth transformation under the solidification of a multicomponent alloy.

4.1. Nucleation model

In the present study we adopted continuous nucleation model in which two different continuous nucleation modes were considered: at the surface (index *s*) and in the bulk (index *b*). The increase of grain density *dn* which corresponds to an undercooling increase $d(\Delta T)$ is described as follows

$$\left(\frac{dn}{d(\Delta T)}\right)_{\varsigma} = \frac{n_{\max,\varsigma}}{\sqrt{2\pi}\Delta T_{\sigma,\varsigma}} \exp\left[-\frac{\Delta T - \Delta T_{\max,\varsigma}}{\Delta T_{\sigma,\varsigma}\sqrt{2}}\right]^2 \tag{6}$$

where: $\Delta T_{\max,s}$, $\Delta T_{\max,b}$, $\Delta T_{\sigma,s}$, $\Delta T_{\sigma,b}$, $n_{\max,s}$ and $n_{\max,s}$ represents the mean nucleation undercooling at the surface, the mean nucleation undercooling in the bulk, the standard deviation at the surface, the standard deviation for the bulk and the maximum density of nuclei that can form in the melt for the surface and bulk, respectively. The local undercooling $\Delta T = T_{liq}(C_1, C_2, ...C_N) - T$ is calculated from the $T_{liq}(C_1, C_2, ...C_N)$ and T from the macroscopic model, defined above.

4.2. Grain growth model

The following model was used as the model of the growth kinetics. The dendrite tip satisfies the Ivantsov solution, and the supersaturation Ω_n is given by

$$\Omega_n = \mathrm{Iv}(\mathrm{Pe}_n);\ \mathrm{Pe}_n = \frac{VR}{2\mathrm{D}_{\mathrm{Ln}}};\ \mathrm{Iv}(\mathrm{Pe}_n) = \mathrm{Pe}_n \exp(\mathrm{Pe}_n)\mathrm{E}_1(\mathrm{Pe}_n) \tag{7,8,9}$$

where $R, \mathrm{D}_{Ln}, \mathrm{Pe}_n, \mathrm{E}_1$ are the dendritic tip radius, the diffusion coefficient of the solute in the liquid, Péclet number and the exponential integral function. Langer and Muller-Krumbhaar [13] have shown that the dendrite tip grows closely to a state called marginally stable. The approximate relationship can be written $R = \lambda_s$, with λ_s is the critical wavelength of the solid-liquid interface at the limit of stability. For multicomponent alloys the wavelength of the marginally stable front is given by the equation [10]

$$\omega^2\Gamma = \sum_{n=1}^{N} m_{vn} G_{c_n} \zeta_{c_n} - \mathrm{G};\ \omega = \frac{2\pi}{R_n};\ m_{vn} = \mathrm{m}_n \left\{1 + \frac{k_n - k_{vn}\left[1 - \ln(k_{vn}/k_n)\right]}{1 - k_n}\right\},$$

$$G_{c_n} = \frac{-V(1-k_{vi})\mathrm{c}_{0n}}{\left[1-(1-k_{vn})\mathrm{Iv}(\mathrm{Pe})\right]D_{Ln}};\quad \zeta_{c_n} = 1 - \frac{2k_{vn}}{\left[1+(2\pi/\mathrm{Pe})^2\right]^{0.5} - 1 + 2k_{vn}} \tag{10,11,12,13,14}$$

where $\omega, m_{vn}, k_{vn}, \mathrm{c}_{0n}, \mathrm{D}_{Ln}, \Gamma, G_{c_n}, \mathrm{G}, \zeta_{c_n}, V$ are the wave number, the velocity dependent liquidus slope of component n, velocity dependent partition coefficient of component n, concentration of component n in the liquid at the dendrite tip, diffusion coefficient of solute in the liquid of component n, Gibbs-Thomson parameter, the concentration gradient of species n in the liquid at the dendritic tip, mean temperature gradient at the interface, stability parameter and the interface velocity, respectively. By using the equation (10) the tip radius can be obtained

$$R_n = 2\pi\Gamma^{0.5}\left(\sum_{n=1}^{N} m_{vn} G_{c_n} \zeta_{c_n} - \mathrm{G}\right)^{-0.5} \tag{15}$$

Several models have been presented to describe the dependence of partition coefficient on velocity. This have been discussed by Boettinger et.al [14]. The Aziz [15] solution for non-equilibrium partition coefficient is used $k_{vn} = (k_n + a_0 V / D_{Ln}) / (1 + a_0 V / D_{Ln})$ where k_n and a_0 are the equilibrium partition coefficient and the characteristic length scale in order of the atomic distance estimated to be

between 0.5 and 5 nm. The tip undercooling can be expressed by the sum of the following undercoolings $\Delta T^* = \Delta T_c + \Delta T_R$ where ΔT_c and ΔT_R are the constitutional and curvature undercooling [16,17] respectively.

$$\Delta T_c = \sum_{n=1}^{N} m_n c_{0n} \left(1 - \frac{m_{vn} / m_n}{1 - (1 - k_{vn}) \mathrm{Iv}(\mathrm{Pe})} \right); \quad \Delta T_K = \frac{2\Gamma}{R_n} \tag{16,17}$$

5. Solution procedures

The solution procedure is as follows. For each slice, the temperature field is solved first, followed by the solution of the concentration fields. Afterwards, the grain structure model is solved, based on the temperature and the concentration fields. The macroscopic fields are assumed to influence the nucleation and the growth of the grains. There is no feedback assumed to take place between the grain growth model and the macroscopic models. The meshless Local Radial Basis Function Collocation Method (LRBFCM) [18] is applied to solve the macroscopic equations (2,3). This method is able to accurately and efficiently solve involved solidification problems such as the turbulent flow [19] with solidification and the macrosegregation as a consequence of the thermosolutal flow [20]. The grain structure model is solved by the Point Automata (PA) technique [16]. This method is similar to the cellular automata method. However, the behaviour is generated by the pre-defined rules based on the local relationship between the nearest neighbouring random points that cover the domain instead of the neighbouring cells. Each random node seed grows with respect to the neighbourhood configuration which is associated with the position of the neighbouring points which fall into a circle [16] with radius R. It means that each point can contain different number and position of the neighbours, which gives various possibilities of neighbourhoods. The detailed description of this novel method can be found in [11, 16]. The KGT model is used as the model of the growth kinetics. Equation (10) is solved numerically by using the false position method. By simultaneously solving equations (10) together with (11), (12), (13), (14) and (15) the variation of Péclet number with the growth velocity V can be calculated. Finally, the relationship between the tip undercooling (16), (17) and the growth velocity can be obtained. The undercooling ΔT is interpolated from the macro model for each random node separately in order to find the growth velocity.

Table 1. Nucleation parameters

quantity		value	unit
mean surface nucleation undercooling	$\Delta T_{\max,s}$	0.6	K
mean bulk nucleation undercooling	$\Delta T_{\max,b}$	12	K
standard deviation for the surface area	$\Delta T_{\sigma,s}$	0.2	K
standard deviation for the bulk area	$\Delta T_{\sigma,b}$	0.5	K

The slice is covered by uniform rectangular 140 x 140 macroscopic node arrangement and approximately 20 random PA points are associated with each macroscopic node. The nucleation, macrosegregation, and ECT/CET model parameters are presented in table 1 and table 2.

6. Validation

The boundary conditions and material properties in the present paper have been made simple in order to put focus on the principle structure of the model and to allow for recalculation of the results. The realistic boundary conditions of the billet caster are described in details in [3,7]. The heat transport in the mould takes into account the heat transport mechanisms through the casting powder, across the air-gap (if it exists), to the mould surface, in the mould, and to the mould cooling water. The heat transport mechanisms in the secondary cooling zone take into account the effects of the casting

velocity, strand surface temperature, spray nozzle type, spray water flow, temperature and pressure, radiation and cooling through the rolls contact. The mentioned basic heat transfer mechanisms are modified with regard to running water and rolls stagnant water at relevant positions. The proper response of the thermal model was validated through infrared thermography [22]. A sensitivity study of the parameters of the grain structure model for Fe-C steel was performed in [7] regarding the macroscopic model, and in [16] regarding the microscopic model. The proper qualitative response of the macrosegregation model was represented in [8] for Fe-C steel.

Table 2. The physical parameters used in calculations [21]

quantity		value	unit
liquidus temperature	T_{liq}	1755.0	K
initial concentration of carbon	c_{0C}	0.510	wt.%
initial concentration of nickel	c_{0Ni}	0.105	wt.%
initial concentration of chromium	c_{0Cr}	1.091	wt.%
partition coefficient for carbon	k_C	0.34	-
partition coefficient for nickel	k_{Ni}	0.9	-
partition coefficient for chromium	k_{Cr}	0.860	-
slope of the liquidus line with respect to the C concentration	m_C	-62.3	K/ wt.%
slope of the liquidus line with respect to the Ni concentration	m_{Ni}	-3.2	K/ wt.%
slope of the liquidus line with respect to the Cr concentration	m_{Cr}	-1.8	K/ wt.%
diffusion coefficient in liquid for C	D_{LC}	$2x10^{-9}$	m^2s^{-1}
diffusion coefficient in liquid for Ni	D_{LNi}	$4.92x10^{-9}$	m^2s^{-1}
diffusion coefficient in liquid for Cr	D_{LCr}	$2.67x10^{-9}$	m^2s^{-1}
Gibbs-Thomson coefficient	Γ	$1.9\ x10^{-7}$	Km
length scale for solute trapping	a_0	$5x10^{-9}$	m

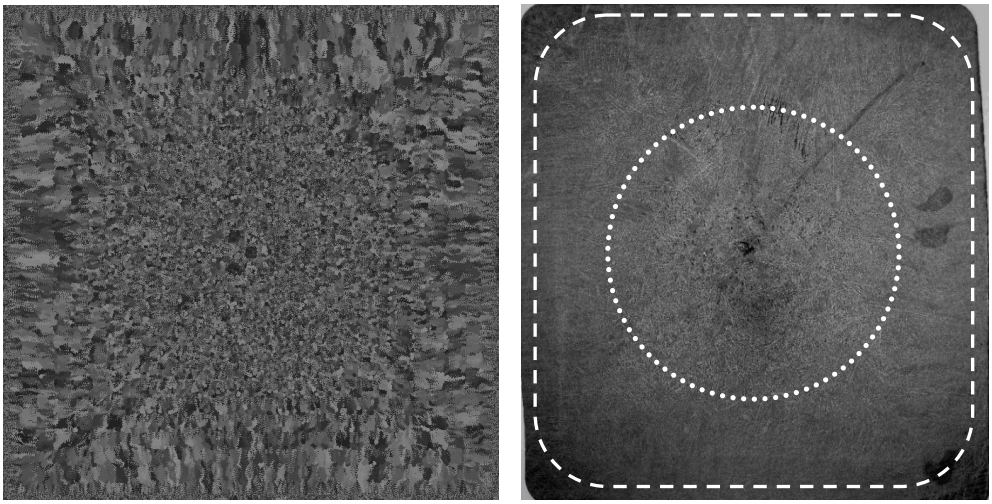

Figure 3. Left: simulated grain structure, and right: Baumann print of the 51CrV4 steel billet.

Figure 3 shows reasonable agreement between calculated (left) and measured (right) grain structure. The primary austenite grain size was between 5 and 7, measured according to standard ASTM E 112.

7. Conclusions

A new, simple slice model for estimating macrosegregation and grain structure in continuously cast strand is represented in the present paper. The model has been demonstrated for billet with 140 mm side and Fe-C-Cr-Ni alloy. A reasonable agreement with the expected macrosegregation and experimental grain structure has been achieved. The model can be used for higher component steel grades as well. The main feature of the model is its simplicity (of course on the expense of accuracy) and related efficiency, which allows the model to be used also in the on-line mode in the perspective. The influence of the fluid flow on macrosegregation is taken into account through artificially increased liquid diffusion coefficient, which mimics the advection of solute enriched liquid steel from the mushy region to the liquid sump in the slice center. The developed model will be used in order to graphically show the on-line status of the strand as well as to provide the data for the plant automation [3]. The coupling, harmonization and further experimental verification of the represented modules with respect to other steel grades, as well as bloom and slab formats is the subject of our future investigations.

Acknowledgement: The present work was supported from the Slovenian Research Agency through grant L2-3651, Slovenian - Montenegro bilateral project SI-CG4-2012/13 and Štore Steel company. The Centre of Excellence for Biosensors, Instrumentation and Process Control is an operation financed by the European Union, European Regional Development Fund and Republic of Slovenia, Ministry of Higher Education, Science and Technology. The financial support is kindly acknowledged.

Reference

[1] Irwing W R 1993 *Continuous Casting of Steel* (London: The Institute of Materials)
[2] Thomas B G 2002 Modeling of the Continuous Casting of Steel - Past, Present Future, www.brimacombecourse.org/pdf/2001_Thomas.pdf
[3] Šarler B, Vernik R, Šaletić S and Cesar J 2005 *Berg- Huettenmaenn. Monatsh*. **150** 300
[4] Louhenkilpi S 2003 *Materials Science Forum* **414-415** 445.
[5] Chaudhary R C, Ji C, Vanka S P and Thomas B G 2011 *Metall. Trans.* **42B** 987
[6] Dantzig J A and Rappaz M 2009 *Solidification* (Lausanne: EPFL Press).
[7] Lorbiecka A Z, Vertnik R, Gjerkeš H, Manojlović G, Senčič B, Cesar J, and Šarler B 2009 *Computers, Materials & Continua* **8** 195
[8] Vušanović I, Vertnik R and Šarler B 2011 *IOP: Conf. Series*: *Mat. Sci. Eng.* **27** 012056
[9] Bennon W D and Incropera F P 1987 *International Journal of Heat and Mass Transfer* **30** 2161
[10] Kurz W and Fisher D J 1981 *Acta metall*. **29** 11
[11] Lorbiecka A Z and Šarler B 2011 *Cellular Automata: Innovative Modelling for Science and Engineering* ed Alejandro (Rijeka) InTech p 197
[12] Lin X, Li Y, Wang M, Feng L, Chen J and Huang W 2003 *Science in China* **46** 475
[13] Langer J S and Muller-Krumbhaar H 1985 J. Cryst. Growth **72** 578
[14] Boettinger W J, Shechtman D, Schaefer R J and Biancaniello F S 1984 Metall. Trans. **15A** 55
[15] Aziz M J 1982 J. Appl. Phys. **53** 1158
[16] Lorbiecka A Z and Šarler B 2009 3rd International Conference of Simulation and Modelling of Metallurgical Processes in Steelmaking, ed A Ludwig (Leoben, Austria) p 192
[17] Lorbiecka A Z, Šarler B., 2010 Computers, Materials & Continua **18** 69
[18] Šarler B and Vertnik R 2006 *Computers and Mathematics with Applications* **51** 1269
[19] Vertnik R and Šarler B 2011 *Adv. Appl. Math. Mech*. **3** 259
[20] Kosec G, Založnik M, Šarler B and Combeau H 2011 *Computers, Materials & Continua* **22** 156
[21] Vannier I, Combeau H and Lesoult G 1993 Materials Science and Engineering A173 317
[22] Gjerkeš H, Šarler B and Vertnik R 2009 3rd International Conference of Simulation and Modelling of Metallurgical Processes in Steelmaking, ed A Ludwig (Leoben, Austria) p 206